

# 1 Annual high-resolution grazing intensity maps on the 2 Qinghai-Tibet Plateau from 1990 to 2020

3 Jia zhou<sup>1,2</sup>, Jin Niu<sup>3</sup>, Ning Wu<sup>1</sup>, Tao Lu<sup>1\*</sup>

4 <sup>1</sup>Chengdu Institute of Biology, Chinese Academy of Sciences, Chengdu 610041, China

5 <sup>2</sup>University of Chinese Academy of Sciences, Beijing 100049, China

6 <sup>3</sup>Department of Economics, Brown University, Providence, 02912, USA

7 *Correspondence to:* Tao Lu ([lutao@cib.ac.cn](mailto:lutao@cib.ac.cn))

8 **Abstract.** Grazing activities constitute the paramount challenge to grassland conservation over the  
9 Qinghai-Tibet Plateau (QTP), underscoring the urgency for obtaining detailed extent, patterns, and  
10 trends of grazing information to access efficient grassland management and sustainable development.  
11 Here, to inform these issues, we provided the first annual Gridded Dataset of Grazing Intensity maps  
12 (GDGI) with a resolution of 100 meters from 1990 to 2020 for the QTP. Five most commonly used  
13 machine learning algorithms were leveraged to develop livestock spatialization model, which spatially  
14 disaggregate the livestock census data at the county level into a detailed 100 m× 100 m grid, based on  
15 seven key predictors from terrain, climate, vegetation and socio-economic factors. Among these  
16 algorithms, the extreme trees (ET) model performed the best in representing the complex nonlinear  
17 relationship between various environmental factors and livestock intensity, with an average absolute  
18 error of just 0.081 SU/hm<sup>2</sup>, a rate outperforming the other models by 21.58%~414.60%. By using the  
19 ET model, we further generated the GDGI dataset for the QTP to reveal the spatio-temporal  
20 heterogeneity and variation in grazing intensities. The GDGI indicates grazing intensity remained high  
21 and largely stable from 1990 to 1997, followed by a sharp decline from 1997 to 2001, and fluctuated  
22 thereafter. Encouragingly, comparing with other open-access datasets for grazing distribution on the  
23 QTP, the GDGI has the highest accuracy, with the determinant coefficient ( $R^2$ ) exceed 0.8. Given its  
24 high resolution, recentness and robustness, we believe that the GDGI dataset can significantly enhance  
25 understanding of the substantial threats to grasslands emanating from overgrazing activities.  
26 Furthermore, the GDGI product holds considerable potential as a foundational source for other  
27 researches, facilitating rational utilization of grasslands, refined environmental impact assessments, and  
28 the sustainable development of animal husbandry. The GDGI product developed in this study is  
29 available at <https://doi.org/10.5281/zenodo.10851119> (Zhou et al., 2024).

## 30 **1 Introduction**

31 Livestock is a crucial contributor to global food systems through the provision of essential animal  
32 proteins and fats, and plays a significant role in supporting human survival and socio-economic  
33 development (Gilbert et al., 2018; Godfray et al., 2018; Humpenöder et al., 2022; Kumar et al., 2022).  
34 However, the escalating increase in human demand for meat and dairy products over recent decades has  
35 triggered a livestock boom, which in turn has increasingly threatened grassland ecosystems and placed  
36 a heavy burden on the environment through overgrazing and land-use change (Tabassum et al., 2016;  
37 Wei et al., 2022; Minoofar et al., 2023). It is estimated that up to 300 million hectares of land are used  
38 globally for grazing and cultivating fodder crops (Tabassum et al., 2016). Grazing activities could alter  
39 vegetation phenology and community structure (Dong et al., 2020), and trigger deforestation  
40 (García-Ruiz et al., 2020), grassland degradation (Sun et al., 2020), soil erosion (Shakoor et al., 2021),  
41 and associated direct releases in greenhouse gas that lead to climate change feedback (Godfray et al.,  
42 2018; Chang et al., 2021). Additionally, livestock are responsible for large-scale dispersion of pathogens,  
43 organic matter, and residual medications into soil and groundwater, thereby contaminating the  
44 environment (Venglovsky et al., 2009; Tabassum et al., 2016; Hu et al., 2017; Muloi et al., 2022).  
45 Consequently, more and more scholars have called attention to provide reliable contemporary dataset to  
46 illustrate the spatio-temporal heterogeneity and variation of livestock (Petz et al., 2014; Fetzel et al.,  
47 2017; Zhang et al., 2018; Li et al., 2021).

48 One of the major challenges in monitoring grazing activity at regional or even larger scale, is the  
49 determination of the livestock distribution pattern. Despite the importance of geographical grazing  
50 information, high spatio-temporal grazing dataset remain unavailable, posing the most critical challenge  
51 to grassland management, particularly for vulnerable grassland ecosystems in fragile regions grappling  
52 with economic and sustainable development contradictions (Miao et al., 2020; Pozo et al., 2021; He et  
53 al., 2022; Meng et al., 2023). In the early 2000s, the Food and Agriculture Organization of the United  
54 Nations (FAO) launched the Gridded Livestock of the World (GLW) project to facilitate a detailed  
55 evaluation of livestock production, aiming to provide pixel-scale livestock densities instead of traditional  
56 administrative unit benchmarks (Nicolas et al., 2016). Consequently, the world's inaugural dataset of  
57 livestock spatialization map (GLW1) was released in 2007, providing the first globally standardized  
58 livestock density distribution map at a spatial resolution of 0.05 decimal degrees ( $\approx 5$  km at the equator)  
59 for 2002. It was not until 2014 that an updated GLW2 map with a 1 km resolution for 2006 was  
60 released, by using a stratified regression approach, superior spatial resolution predictor variables, and  
61 more detailed livestock census data (Robinson et al., 2014). Furthermore, an evolutionary step in  
62 machine learning technology saw Gilbert et al. (2018) using random forests algorithm to forge a global  
63 livestock distribution map with a 10-km resolution for 2010 (GLW3), succeeding traditional multivariate  
64 regression methods and surpassing the precision of previous GLW1 and GLW2 maps. Beyond these  
65 global mappings, several maps with different scales have also been published, including intercontinental,  
66 national, state or provincial, and local scale (Neumann et al., 2009; Prosser et al., 2011; Van Boeckel  
67 et al., 2011; Nicolas et al., 2016). However, these maps are fundamentally coarse due to constraints such as  
68 the availability of fine scale and contemporary census data, the grazing spatialization method, as well as  
69 the identification of appropriate indicators, thereby limiting their application to local or regional-scale  
70 studies (Robinson et al., 2014; Nicolas et al., 2016; Gilbert et al., 2018). Hence, there is an emergent  
71 demand for more refined grazing map products (Mulligan et al., 2020; Martinuzzi et al., 2021).

72 An exemplar of this need can be observed in the Qinghai-Tibet Plateau (QTP), the world's most

73 elevated pastoral region and an important grazing area in China (Zhan et al., 2023). It was possessing  
74 abundant grassland that spans 1.5 million km<sup>2</sup>, accounting for 50.43% of China's total grassland area,  
75 with Yak and Tibetan sheep as primary grazing livestock (Feng et al., 2009; Cai et al., 2014; Zhan et al.,  
76 2023). Over recent decades, the QTP has undergone escalating grassland degradation, leading to many  
77 ecological and socio-economic problems, which calls for an urgent need for detailed livestock  
78 distribution dataset (Li et al., 2022a). Unfortunately, despite researchers' efforts at mapping the QTP's  
79 grazing intensity, current livestock dataset still suffer from coarse spatio-temporal resolution and  
80 modelling accuracy. Apart from the aforementioned global grazing dataset, several other maps also  
81 cover the QTP. For instance, Liu et al. (2021) generated annual 250-m gridded carrying capacity maps  
82 for 2000-2019, by employing multiple linear regressions of livestock numbers, population density, NPP,  
83 and topographic features. Li et al. (2021) used machine learning algorithms to produce gridded livestock  
84 distribution data at 1 km resolution for 2000-2015 in western China at five year interval, based on  
85 county-level livestock census data and 13 factors from land use practice, topography, climate, and  
86 socioeconomic aspects, including grassland coverage, arable land coverage, forest land coverage, desert  
87 coverage, NDVI, elevation, slope, daytime surface temperature, precipitation, distance to river, travel  
88 time to major cities, population density, and GDP (Li et al., 2021). A contribution from Meng et al.  
89 (2023) brought forth annual longer time-series grazing maps by using random forests model, integrating  
90 climate, soil, NDVI, water distance, and settlement density to decompose county-level livestock census  
91 data to a 0.083° (≈10 km at the equator) grid for 1982-2015 (Meng et al., 2023). Similarly, Zhan et al.  
92 (2023) also used random forests algorithm to combine eleven influence factors to provide a winter and  
93 summer grazing density map at 500 m resolution for 2020 (Zhan et al., 2023).

94 However, although these maps have provided good help in understanding grazing conditions on the  
95 QTP, there are currently still no maps that can satisfy the need for fine-scale grassland management  
96 with a long time span. In addition, the available livestock distribution maps of the QTP still need  
97 improvement in terms of modelling techniques and factor selection to obtain high-precision livestock  
98 spatialization data. For example, traditional methods like multiple linear regression, while proven  
99 fundamental and widely applicable for livestock spatialization (Robinson et al., 2014; Ma et al., 2022),  
100 are being challenged by the development of computational science in recent years. Among them,  
101 machine learning technology is providing new opportunities towards more accurate predictions of  
102 livestock distribution (García et al., 2020). Random forests regression, for instance, is currently widely  
103 used to construct global, national as well as regional livestock spatialization dataset, and has been proved  
104 to have much better accuracy than traditional mapping techniques (Rokach, 2016; Nicolas et al., 2016;  
105 Gilbert et al., 2018; Chen et al., 2019; Dara et al., 2020; Li et al., 2021). Nevertheless, other more  
106 advanced machine learning methods with superior feature learning and more robust generalization  
107 capabilities, remains largely untapped for modelling geographic data (Ahmad et al., 2018; Heddami et al.,  
108 2020; Long et al., 2022). Thus, exploring the potential application of new advanced machine learning  
109 technologies in livestock spatialization remains a critical task. Furthermore, selecting the suitable factors  
110 that influencing livestock grazing preferences is also the other critical challenge for enhancing the  
111 precision of grazing distribution dataset (Meng et al., 2023). Livestock grazing activities are often  
112 affected by abiotic and biotic resources, including climatic and environmental factors (Waha et al.,  
113 2018), herd foraging and grazing behaviours (Garrett et al., 2018; Miao et al., 2020), and  
114 conservation-oriented policies (Li et al., 2021). For instance, regions exceeding elevations of 5,600 m or  
115 slope greater than 40% are customarily unsuitable for grazing (Luo et al., 2013; Mack et al., 2013;  
116 Robinson et al., 2014; Chen et al., 2019). Moreover, the livestock generally prefer areas abundant in

117 water and pasture resources for foraging (Li et al., 2021). Besides, ecological conservation policies also  
118 exert substantial influence, significantly affecting grazing distribution relative to the level of  
119 conservation priority. In addition, the health status of the grassland is an important factor influencing  
120 whether livestock choose to feed or not (Li et al., 2021). Consequently, indicators related to the above  
121 aspects are often employed to gauge the spatial heterogeneity of livestock distribution (Allred et al.,  
122 2013; Sun et al., 2021; Meng et al., 2023). Nonetheless, some most commonly used indicators like NPP  
123 or NDVI can result in misconceptions, as they may not fully characterize the grazing intensity. For  
124 example, grasslands with high NPP or NDVI are often preferred by livestock, but this doesn't necessarily  
125 correlate with grazing intensity in nature reserves due to strict policy restrictions (O'Neill and Abson,  
126 2009; Veldhuis et al., 2019; Zhang et al., 2021b). Conversely, areas with sparse grassland cover may  
127 support considerable livestock numbers, despite evidence of degradation (Guo et al., 2015; Zhang et al.,  
128 2021a). Accordingly, further investigation of novel indicators is imperative to enhance the correlation  
129 between grassland and grazing intensity, thereby optimizing the integration of such influencing factors  
130 into grazing spatialization models.

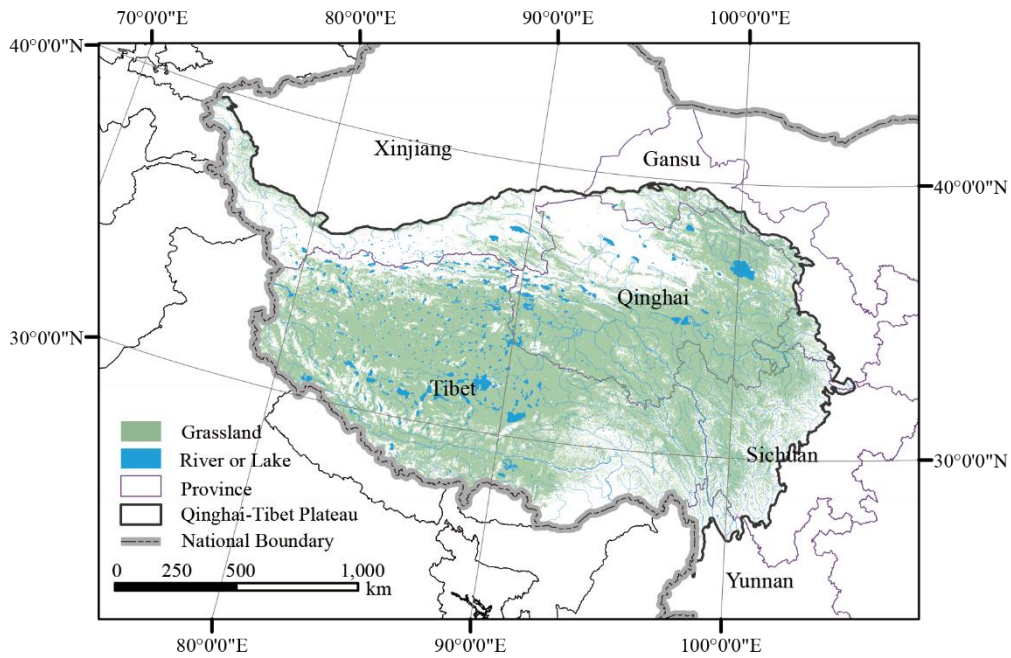
131 In summary, the QTP is in pressing need for a high spatio-temporal resolution grazing dataset to  
132 address urgent and realistic challenges. But the existing livestock dataset specific to the QTP are fraught  
133 with several insufficient, predominantly concerning rough resolution, relatively backward census data,  
134 as well as conventional methods in livestock spatialization. Moreover, the discrepancies in predictive  
135 indicators and modelling approaches within these dataset discourage their application in time-series  
136 analysis. Consequently, the generation of high-resolution and high-quality grazing map products has  
137 emerged as the most pressing challenge for the QTP. Here, we aim to (1) establish a methodological  
138 framework by using more rational models and indicators than traditional studies to achieve fine-scale  
139 livestock spatialization; (2) select the grazing spatialization model with good performance by  
140 incorporating multi-source data with advanced machine learning techniques; and (3) ultimately, provide  
141 an annual grazing intensity dataset with 100 m resolution spanning from 1990-2020. These maps can not  
142 only provide fundamental dataset with finer spatio-temporal resolution to address the limitations of  
143 existing grazing intensity maps, but enhance a better understanding of sustainable management practices  
144 as well as other grassland-related issues across the QTP.

## 145 **2 Data and methods**

### 146 **2.1 Study area**

147 Known as the Asia's water tower and the world's third pole, the QTP is geographically situated  
148 between 73°19'~104°47' east longitude and 26°00'~39°47' north latitude, with a total area of about 2.61  
149 million square kilometers (Figure 1). Its jurisdiction encompasses 182 counties within six provincial  
150 regions of China, including Tibet Autonomous Region, Qinghai Province, Xinjiang Uygur Autonomous  
151 Region, Gansu Province, Sichuan Province, and Yunnan Province (Meng et al., 2023). Elevation on the  
152 QTP predominantly ranges between 3,000 m and 5,000 m, with an average altitude exceeding 4,000 m.  
153 With grasslands constituting over half of its land cover, the QTP emerges as one of the most important  
154 pastoral areas in China. Alpine steppe, alpine meadow, and temperate steppe characterize the main  
155 grassland types on the QTP (Han et al., 2019; Zhai et al., 2022; Zhu et al., 2023a). The complex  
156 geographical and climatic conditions of the QTP contributes to the markedly heterogeneous grassland  
157 distribution, which correspondingly lead to the high heterogeneity in livestock distribution. Moreover,  
158 social and economic development, coupled with policy initiatives directed towards grassland restoration,

159 have noticeably impacted the livestock numbers on the QTP over recent decades (Li et al., 2016; Li et al.,  
160 2021).



161 Figure 1. The geographic zoning map of the Qinghai-Tibet Plateau (QTP) superposed with grassland vegetation.  
162 Boundaries for the six provinces used for statistical analysis are also shown.

## 163 2.2 Data source

### 164 2.2.1 Census livestock data

165 The county-level census livestock data for the period between 1990 and 2020 were obtained from  
166 the Bureau of Statistics of each county across the QTP. The data includes the number of cattle, sheep,  
167 horse and mule, with the exception of counties in Yunnan Province, which lack data for the years from  
168 1990 to 2007, and Ganzi Prefecture in Sichuan Province, which lack data for the years from 1990 to  
169 1999, and Muli county in Sichuan Province, which lack data for the years from 1990 to 2007. For these  
170 counties belonging to the same prefecture, including counties in Ganzi and Aba prefectures in Sichuan  
171 Province, we used the livestock census data at the prefecture-level to carry out spatialization. For these  
172 counties in Yunnan Province, since they belong to different municipalities, it is not reasonable to  
173 replace them with municipal-level data. For these counties without livestock census data for some years,  
174 we Supplementaryed the missing data by linear interpolation with grazing density data in available year.  
175 In total, livestock data were available for 182 counties, and 4,998 independent records were finally  
176 generated. Furthermore, the respective quantities of different livestock types are converted to Standard  
177 Sheep Units (SU), in compliance with the Chinese national regulations (Meng et al., 2023).

178 Due to the difficulty of collecting township-level census livestock data, the validation data at the  
179 township scale collected in this study only involved these townships of Baching County (2010-2018)  
180 and Gaize County (2018-2020) in Tibet, and Hongyuan County in Sichuan Province (2008). The  
181 township-level census livestock data cumulatively involves 18 townships with a total of 112 records,  
182 and were only used for auxiliary validation of the simulation results.

183 The validation data at the pixel scale also encompass a total of 112 records from 68 sites, which  
184 were collected from literatures, questionnaires and field surveys. Specifically, 93 records at 49 sites

185 spanning the 1990-2020 period were obtained from 17 literatures, 19 records at 19 sites were obtained  
186 from the questionnaires and the field survey in 2021. The detailed information for these records can be  
187 found in the Supplementary files (Figure S3 and Table S3).

### 188 *2.2.2 Factors affecting grazing activities*

189 In this study, topography, climatic, environmental and socio-economic impacts were considered as  
190 influential factors on grazing activities (Li et al., 2021; Meng et al., 2023). Accordingly, altitude, slope,  
191 distance to water source, population density, air temperature, precipitation and human-induced impacts  
192 on NPP (HNPP) was selected as indicators. Specifically, elevation is derived from the DEM dataset  
193 accessible via the Resource and Environmental Data Cloud Platform of the Chinese Academy of  
194 Sciences (<https://www.gscloud.cn>), which also facilitated slope calculation. Rivers and lakes were  
195 obtained from the National Tibetan Plateau Data Center (<https://data.tpdc.ac.cn>), and the nearest  
196 Euclidean distance from each pixel to rivers or lakes is calculated accordingly. Meteorological elements  
197 such as daily air temperature and precipitation were downloaded from the China Meteorological Data  
198 Service Center (<http://data.cma.cn>). For the grid dataset that is not conditionally available, including  
199 population density, temperature, precipitation and HNPP, we detailed the creation process in the  
200 Supplementary file. All datasets utilized in this study were harmonized to consistent coordinate  
201 systems and resolutions (WGS 1984 Albers, 100 m).

### 202 **2.3 Methodological framework**

203 We adopted a comprehensive methodological framework for mapping high-resolution grazing  
204 intensity on the QTP. Three major steps are included to predict the distribution pattern of grazing  
205 intensity: (1) identifying factors affecting grazing activities and extracting theoretical suitable areas for  
206 livestock grazing, (2) building grazing spatialization model, and (3) filtering the model and correcting  
207 the grazing map. An exhaustive explanation of each step is provided in Figure 2.

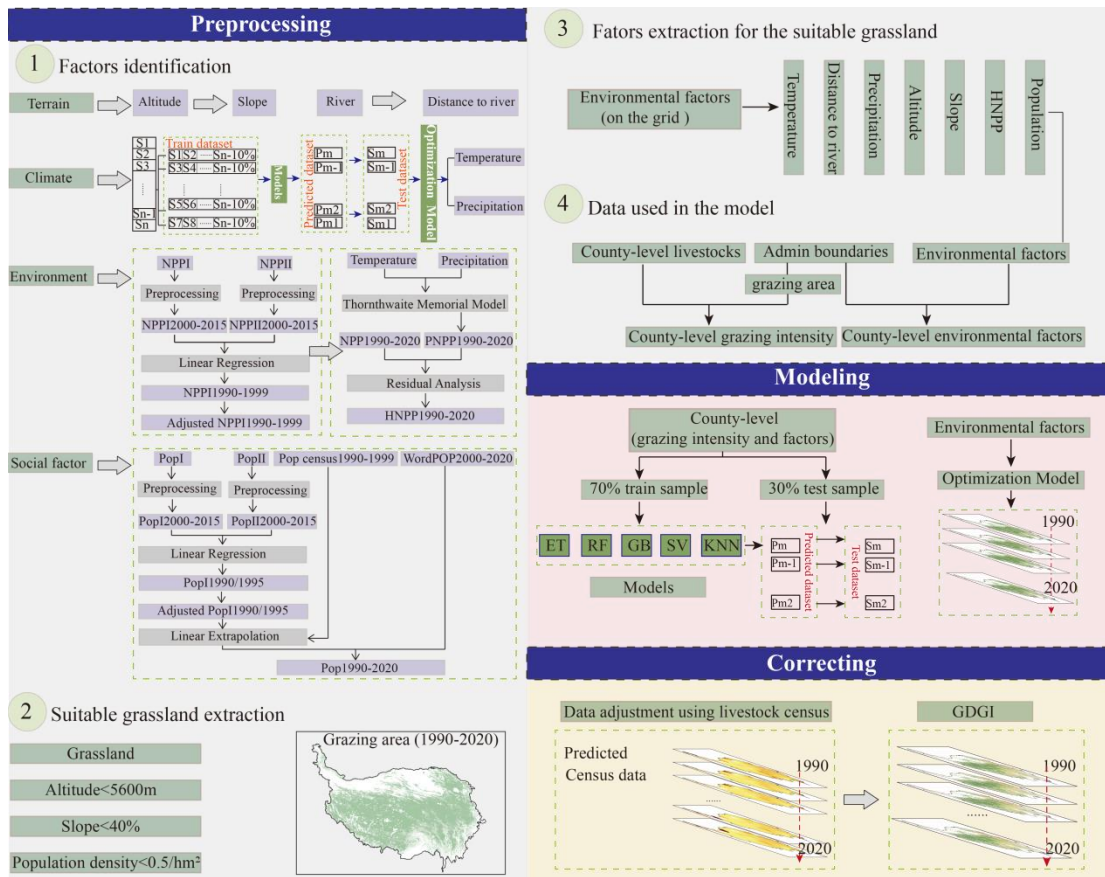


Figure 2. Flowchart of creating grazing intensity maps using different methods and source products.

### 2.3.1 Identifying factors and theoretical suitable areas for grazing

In this study, we assumed that grazing activities are confined solely to grassland. Consequently, the potential grazing areas for each year were identified on the basis of grassland boundaries, which was extracted from the 30 m annual land cover dataset (CLCD) (Yang and Huang, 2021). Furthermore, grassland with slope over 40% and elevation higher than 5,600 m respectively, were considered unsuitable for grazing and were therefore excluded from the potential grazing area in the subsequent simulations (Robinson et al., 2014). In addition, the grassland with population density greater than 50 inhabitants km<sup>-2</sup> were also excluded. The remaining isolated grassland was thus categorized as theoretical feasible grazing regions.

The spatial patterns of abiotic and biotic resources, incorporating food availability, environmental stress, and herder preference critically affect grazing activities (Meng et al., 2023). In light of this, seven influencing factors in four aspects were selected for grazing intensity mapping (Figure 2-1).

### 2.3.2 Building grazing spatialization model

By performing regional statistics, the annual average values for each grazing influence factor were extracted from the theoretically suitable grazing areas at the county scale, and were further used as independent variables in the model construction. The dependent variable for the model was acquired by determining the livestock density within each county, followed by a logarithmic transformation of the values to normalize the distribution of the dependent variable. Consequently, a total of 4,998 samples were derived from the aforementioned independent and dependent variables. Of these samples, 70%

229 were allocated for model training, while the remaining 30% comprised the test sets, serving to validate  
 230 the model's performance. Subsequently, we built grazing spatialization models using five machine  
 231 learning algorithms at the county scale, including Support Vector regression (SV) (Cortes and Vapnik,  
 232 1995; Lin et al., 2022), K-Nearest Neighbors (KNN) (Cover and Hart, 1967), Gradient Boosting  
 233 regression (GB) (Friedman, 2001; Pan et al., 2019), Random Forests (RF) (Breiman, 2001) and Extra  
 234 Trees regression (ET) (Geurts et al., 2006; Ahmad et al., 2018) (see Supplementary file for details).  
 235 Lastly, to assess the accuracy of the spatialized livestock map, the predicted livestock intensity values  
 236 were juxtaposed with the livestock statistical data from each respective county.

### 237 2.3.3 Correcting the grazing map

238 We further used the optimal model to predict the geographical distribution of grazing density across  
 239 the QTP. To maintain better consistency between the predicted livestock number and the census data,  
 240 the estimated results were adjusted using the census livestock numbers at the county scale as a control  
 241 according to Equation (1). Consequently, the corrected and refined map is presented as the final grazing  
 242 intensity map in this study.

$$243 \quad L_{correction} = \frac{L_{CCensus}}{L_{Cgrid}} \times L_{grid} \quad (1)$$

244 where  $L_{correction}$  is the predicted pixel-scale livestock number after adjustment,  $L_{Cgrid}$  represents the  
 245 estimated livestock number for each county,  $L_{CCensus}$  is the census livestock number for each county,  
 246 and  $L_{grid}$  refers to the predicted livestock number at the pixel scale.

### 247 2.4 Accuracy evaluation

248 We used three accuracy validation indexes to evaluate the performance of five machine learning  
 249 algorithms, including coefficients of determination ( $R^2$ ), mean absolute error (MAE), and root mean  
 250 square error (RMSE), by through a comparison of the predicted value with the census data. The  
 251 definitions of three metrics are presented in Equation (2)~(4).

$$252 \quad R^2 = 1 - \frac{\sum_{i=1}^n (C_i - P_i)^2}{\sum_{i=1}^n (C_i - \bar{C})^2} \quad (2)$$

$$253 \quad MAE = \frac{1}{n} \sum_{i=1}^n |C_i - P_i| \quad (3)$$

$$254 \quad RMSE = \sqrt{\frac{1}{n} \sum_{i=1}^n (C_i - P_i)^2} \quad (4)$$

255 where  $C_i$  and  $P_i$  are the census livestock data and the predicted value for county  $i$ , respectively;  $\bar{C}$   
 256 represents the mean census value for all county; and  $n$  gives the total number of counties.

## 257 3 Results

### 258 3.1 Performances of models

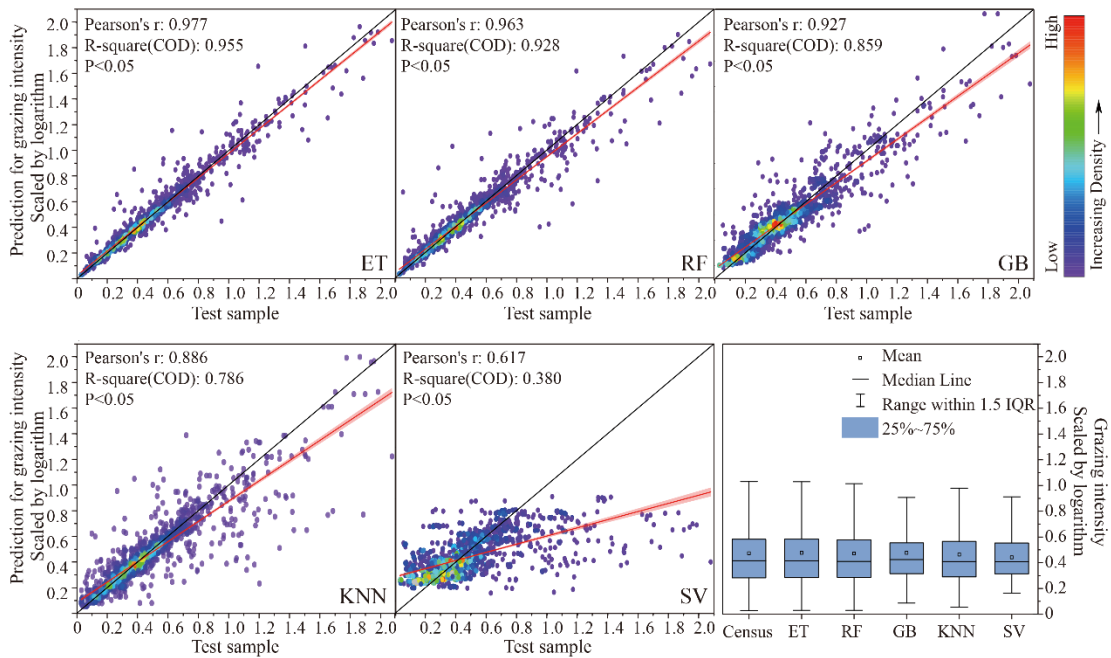
259 Table 1 summarizes the efficiency of the five used machine learning models with considering all  
 260 three accuracy evaluators of  $R^2$ , MAE and RMSE. It can be seen that the ET model performs the best,  
 261 with its  $R^2$  exceeding 0.955, and MAE (0.081 SU/hm<sup>2</sup>) and RMSE (0.164 SU/hm<sup>2</sup>) significantly lower  
 262 than the value of RF, GB, KNN and SVM models. Figure 3 illustrates the correlation between the  
 263 census livestock data and the livestock numbers predicted by the model for each county from 1990 to



264 2020. It demonstrated that the ET-predicted data displayed a distribution pattern consistent with that of  
 265 other models, but the scatter points of the ET model were more convergent to the 1:1 diagonal line,  
 266 indicating a superior fit compared to the other models. These comparisons suggest that the ET model  
 267 possesses superior robustness and can, therefore, provide stable estimations of livestock intensity on  
 268 the QTP.

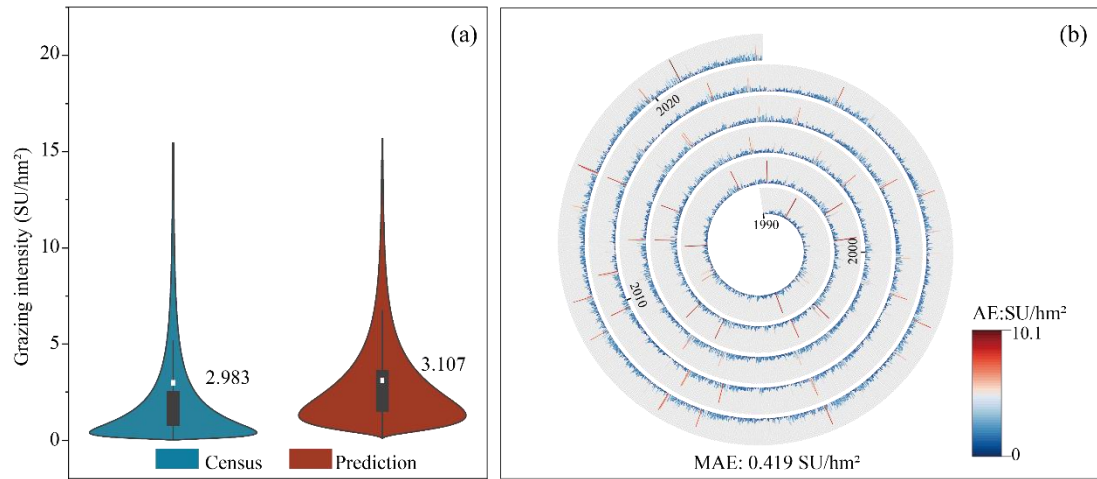
269 Table 1. Comparison of mapping accuracy for five machine learning models based on the same validation datasets

Models	$R^2$	MAE (SU/hm <sup>2</sup> )	RMSE (SU/hm <sup>2</sup> )
ET	0.955	0.081	0.164
RF	0.928	0.099	0.208
GB	0.859	0.197	0.300
KNN	0.786	0.186	0.384
SVM	0.380	0.419	0.750



270  
 271 Figure 3. Scatterplots of model-predicted livestock numbers and census grazing data at the county scale. The red  
 272 solid line and the black solid line are the fitting line and the 1:1 diagonal line, respectively.

273 Utilizing the ET model, we predicted the spatio-temporal distribution of grazing intensity across the  
 274 QTP from 1990 to 2020 with a resolution of 100 m × 100 m. To test the accuracy of these maps, we  
 275 aggregated the prediction results from the pixel level to county level and compared them with the  
 276 livestock census data (Figure 4a). It is evident that the predicted livestock intensity was highly  
 277 consistent with the county-level census data, displaying particular robustness in lower grazing intensity  
 278 scenarios (Figure 4b). Specifically, comparing with 2.983 SU/hm<sup>2</sup> for the mean census data, our  
 279 county-level predicted datasets revealed an average grazing intensity of 3.106 SU/hm<sup>2</sup>, with MAE of  
 280 0.123 SU/hm<sup>2</sup>, RMSE of 0.580 SU/hm<sup>2</sup>, and  $R^2$  of 0.669. Moreover, the data discrepancies for 76.31%  
 281 (number of counties=3,814) were not exceeding 0.6 SU/hm<sup>2</sup>, and 91.74% (number of counties=4,585)  
 282 remaining under 1.0 SU/hm<sup>2</sup>. Finally, employing county-level livestock census data as a benchmark for  
 283 quality control, we obtained the final annual gridded datasets for grazing intensity (GDGI) across the  
 284 QTP spanning 31 years from 1990 to 2020.

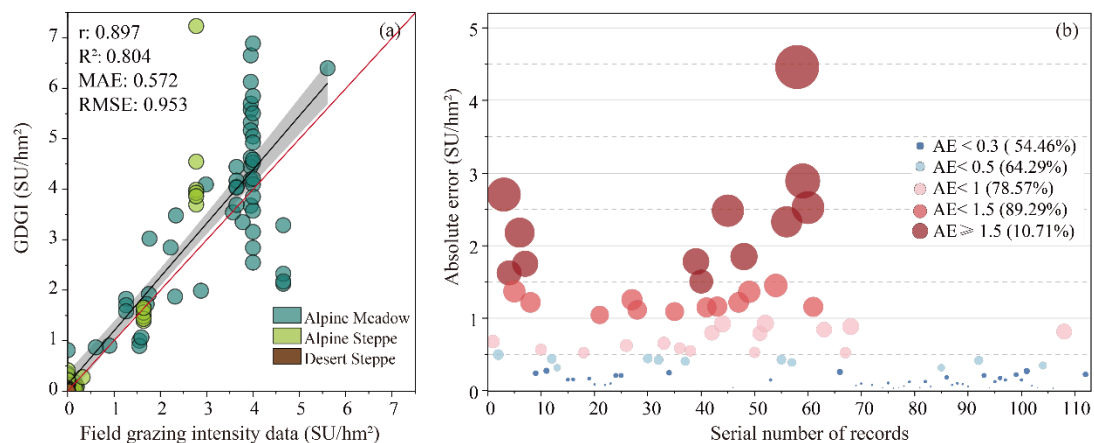


285

286 Figure 4. Accuracy of the ET-predicted grazing intensity results at spatial resolution of 100 m from 1990 to 2020.  
 287 (a) comparison of the predicted value and the census data at the county scale; (b) absolute error for each county.

### 288 3.2 Validation of the GDGI dataset

289 We firstly confirmed the accuracy of the GDGI dataset based on 112 field grazing intensity records  
 290 at 68 sites (see Table S3 in Supplementary file for details), which ranged from 0 to 5.61 sheep unit per  
 291 hectare (SU/hm<sup>2</sup>), and covered three main grasslands on the QTP: the alpine steppe (N=62), alpine  
 292 meadow (N=46), and alpine desert steppe (N=4). The GDGI dataset was assessed by undertaking a  
 293 comparative accuracy assessment between it and the field grazing intensity data (Figure 5a). It can be  
 294 seen that in general, our dataset was highly consistent with the reference ground-truth validation data,  
 295 with  $R^2 = 0.804$ , MAE = 0.572 SU/hm<sup>2</sup>, and RMSE = 0.953 SU/hm<sup>2</sup>. Moreover, the absolute errors  
 296 between the GDGI data and the field grazing intensity data were relatively small, with more than half  
 297 of the records having an error below 0.3 SU/hm<sup>2</sup>, 78.57% below 1.0 SU/hm<sup>2</sup>, and 89.29% below 1.5  
 298 SU/hm<sup>2</sup> (Figure 5b).

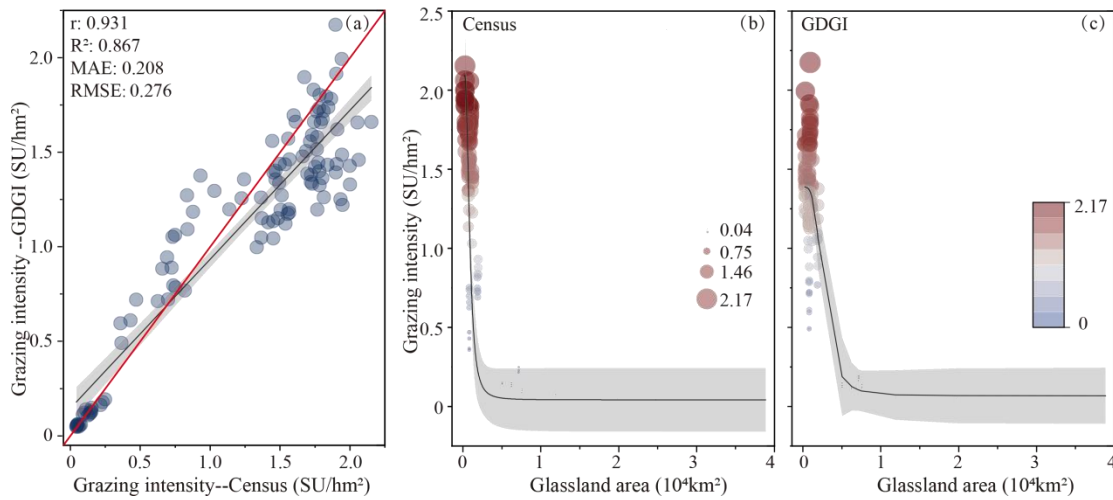


299

300 Figure 5. Validation of the GDGI dataset using 112 field grazing intensity records at the pixel scale: (a) linear  
 301 fitting results; (b) absolute error (AE) distribution.

302 We further validated the precision of the GDGI dataset using the township-level livestock census  
 303 data. Encouragingly, the evaluation results showed that the GDGI dataset has excellent performance at  
 304 the township scale (Figure 6a), with  $R^2$  of 0.867, MAE of 0.208 SU/hm<sup>2</sup>, and RMSE of 0.276 SU/hm<sup>2</sup>.

305 In addition, similarly to the census data, the GDGI dataset indicated that some townships with few  
 306 grassland area are still under high grazing pressure (Figure 6b and 6c).



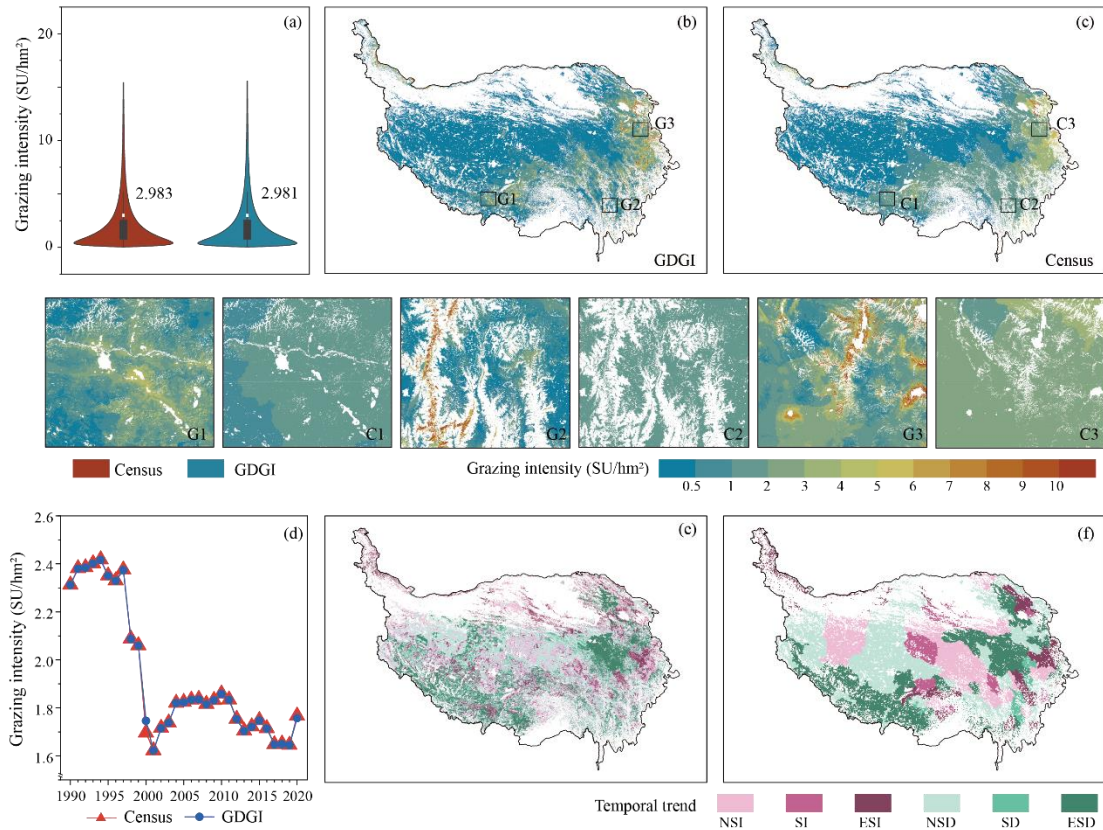
307

308 Figure 6. Validation of the GDGI dataset using census livestock data at the township level: (a) linear fit of  
 309 predicted number and census data; (b-c) logistic fit of grazing intensity data and grassland area.

### 310 3.3 Spatio-temporal variations of grazing intensity

311 In terms of the temporal trends of grazing intensity, the GDGI dataset overall exhibited consistent  
 312 trends with the livestock census data (Figure 7d-7f). Specifically, the census data indicated the  
 313 livestock numbers remained high and largely stable from 1990 to 1997, followed by a sharp decline  
 314 from 1997 to 2001, and then remained a period of fluctuation post-2001, which was successfully  
 315 captured by the GDGI dataset. Moreover, the spatial heterogeneity of grazing intensity within the  
 316 counties over the QTP was also effectively reflected by the GDGI dataset, a characteristic not  
 317 illustrated by the census dataset. For example, areas of high grazing intensity were concentrated in the  
 318 northeastern and south-central regions of the plateau, mainly including the eastern part of Qinghai  
 319 Province, the southwestern part of Gansu Province, the northwestern part of Sichuan Province, and the  
 320 eastern region of the Tibet Autonomous Region (Figure 7e and 7f).

321 Over the past 31 years, 63.95% of the plateau's grassland showed a decreasing trend in grazing  
 322 intensity, with 49.80% showing significant decreases, primarily located in the eastern Sanjiangyuan  
 323 area and the southwestern region of the QTP (Figure 7e and 7f). Meanwhile, grazing intensity was  
 324 increasing in 36.05% of the grassland, but most of them (60.16%) did not reach the level of  
 325 significance and were mainly distributed in the northeastern plateau (Figure 7e and 7f).



326

327 Figure 7. Validation of the GDGI maps using the census grazing data from 1990 to 2020: (a) violin plot of the  
 328 census data and the predicted value; (b-c) spatial distribution in SU per pixel; (d) temporal change in SU per year  
 329 (only including 124 counties with livestock census data); (d-f) spatial distribution of SU changes tested by sen's  
 330 slope and Mann-Kendall. Note: ESI for Extremely Significant Increase (slope>0 & p<0.01); SI for Significant  
 331 Increase (slope>0 & p<0.05); NSI for Non-significant increase (slope>0 & p>0.05); ESD for Extremely  
 332 Significant Decrease (slope<0 & p<0.01); SD for Significant decrease (slope<0 & p<0.05); NSD for  
 333 Non-significant decrease (slope<0 & p>0.05).

#### 334 4 Discussion

##### 335 4.1 Comparison with other grazing intensity maps

336 To further assess the effectiveness and reliability of the developed GDGI dataset, the mapping  
 337 results were juxtaposed with seven publicly available grazing intensity maps covering the QTP (Table  
 338 2). It can be seen that despite their public availability, these maps lacked both in spatial and temporal  
 339 resolution when juxtaposed with the GDGI maps. Our analysis was extended to four openly accessible  
 340 gridded livestock datasets, including GI-Sun (Sun et al., 2021), ALCC (Liu, 2021), GI-Meng (Meng  
 341 et al., 2023) and GLWs (Gilbert et al., 2018). Among the GLW series, GLW3 and GLW4 were chosen  
 342 owing to their superior performances over GLW1 and GLW2, as indicated by Gilbert et al. (2018). A  
 343 commonality among all five maps was the consistency for the spatial patterns of grazing intensity, with  
 344 prevalent high and low intensities in the northeast and northwest regions, respectively (Figure 8).  
 345 However, these maps differed significantly in terms of accuracy. As the grazing intensity maps of  
 346 GLWs and ALCC were produced based on the livestock census data in 2001 and 2015, an accuracy  
 347 comparison for the corresponding years was conducted among the five datasets. It was observed from

348 the scatter diagrams that  $R^2$  between the predicted and livestock statistic data for GI-Sun, ALCC, and  
349 GLWs are lower than 0.6, which is significantly lower than the accuracy of GDGI ( $R^2$  exceeds 0.9)  
350 (Figure 8a). Furthermore, GDGI exhibited the closest to the census data, as evidenced by the fact that  
351 MAE and RMSE are less than 1 (Figure 8b, 8c). Moreover, the GDGI dataset spanning 31 years  
352 (1990-2020) earmarked it as a more suitable choice for long-term studies in comparison to the other  
353 four datasets. Regarding spatial distribution, the overall patterns of these grazing maps are largely  
354 consistent, exhibiting higher density patterns in the southeast and lower in the northwest. However,  
355 notable discrepancies are still apparent in the finer details. In general, in terms of visually representing  
356 the spatial distribution of livestock, the GDGI maps exhibit the best performance.

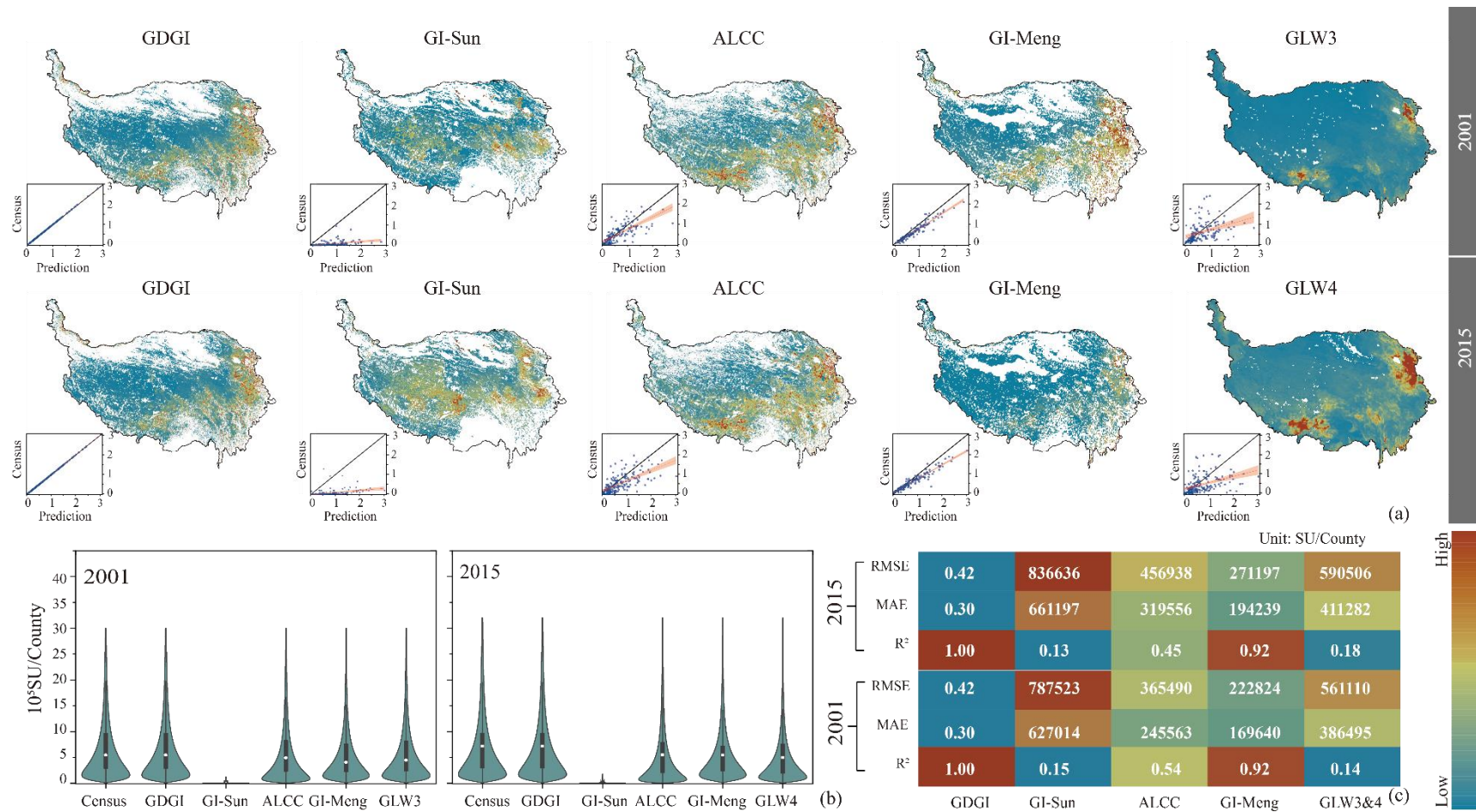
357 The above advantageous of the GDGI dataset are understandable. First, the livestock census data  
358 used in GDGI is more detailed, aiding in enhancing the accuracy of the estimation results. Specifically,  
359 GI-sun, ALCC, GI-Meng and GDGI all use county-level livestock statistics to map grazing intensity,  
360 whereas GLW3 and GLW4 are based on provincial-level census data to map, which results in their  
361 accuracy lagging significantly behind the four other datasets (Nicolas et al., 2016; Sun et al., 2021).  
362 Second, grazing densities are estimated by dividing the number of livestock from the statistical data,  
363 after a mask excluding theoretical unsuitable grazing areas. However, these maps differ in their  
364 definitions of suitable grazing areas. In this study, as with the GI-sun and GI-Meng maps, we  
365 considered grazing to occur only on grasslands, and further excluded unsuitable areas such as high  
366 elevations and steep slopes. This kind of definition is clearly more reasonable than the GLW series,  
367 which removed only water bodies, urban core areas, and protected areas with relatively tight  
368 regulations of human activity (Mcsherry and Ritchie, 2013; He et al., 2022). However, the GI-Meng  
369 dataset considers the core areas of protected areas as grazing-free region, it does not match the actual  
370 situation on the QTP (Zhao et al., 2020; Li et al., 2022b; Jiang et al., 2023). Those different thresholds  
371 for the definition of suitable grazing areas are account for the fact each map has different theoretical  
372 grazing regions. Third, these maps decompose the livestock census data to pixels based on different  
373 mathematical theories, which also leads to differences in prediction accuracy across maps. Specifically,  
374 ALCC used a multivariate linear regression algorithm to predict grazing intensity, which has been  
375 shown to be significantly inferior to the RF machine learning method employed by GI-Meng, GLW3  
376 and GLW4 (Nicolas et al., 2016; Li et al., 2021). In this study, we used the ET model to predict  
377 livestock numbers and achieved higher accuracy accordingly. Finally, differences in the selection of  
378 factors affecting livestock distribution across maps may also lead to differences in map accuracy.  
379 Specifically, GI-sun only used the NPP as indicator, but it is not simply linearly related to grazing  
380 intensity (Gilbert et al., 2018; Sun et al., 2021; Ma et al., 2022). ALCC considered the population  
381 density, NPP, and terrain as indicators, which are also incomplete considerations of the influencing  
382 factors. On the other hand, GLW series dataset considered 12 factors, such as NDVI, EVI, population  
383 distribution and elevation. GI-Meng dataset incorporated 14 factors including NDVI, soil PH, available  
384 nitrogen, available phosphorus, and available potassium. However, GLWs and GI-Meng ignored the  
385 decrease in the prediction accuracy due to redundancy among the factors. In this study, we selected  
386 factors related to grazing activities including terrain, climate, environment and social factor, and  
387 constructed a prediction model with seven factors including population density, elevation, climate, and  
388 HNPP. Unlike other livestock products, this study used HNPP for the first time to replace the  
389 commonly used NPP, or NDVI, or EVI as indicator, which has be proved to be more accurately  
390 expressed the relationship between livestock and grassland (Huang et al., 2022).

391 Table 2. Summary of map-derived parameters for this study and other seven public gridded livestock datasets covering the QTP.

<b>Dataset</b>	<b>Accessibility</b>	<b>Census</b>	<b>Temporal resolution</b>	<b>Spatial resolution</b>	<b>Period (years)</b>	<b>Method</b>	<b>Livestock type</b>
GDGI	Yes	County	annual	100 m	1990-2020 (31)	ET	Standard SU
GLW3	Yes	Province/sub-Province	annual	0.083°(≈10 km)	2001 (1)	RF	Cattle, ducks, pigs, chickens,
GLW4	Yes	Province/sub-Province	annual	0.083°(≈10 km)	2015 (1)	RF	sheep, goats
GI-Sun	Yes	County	five-year interval	1 km	1990-2015 (6)	LRA	Standard SU
ALCC	Yes	Province/sub-Province	annual	250 m	2000-2019 (20)	MLR	Standard SU
GI-Meng	Yes	County	annual	0.083°(≈10 km)	1982-2015 (34)	RF	Standard SU
GI-Li	No	County	five-year interval	1 km	2000-2015 (4)	DNN	Cattle and sheep
GI-Zhan	No	County	season	15'' (≈500 m)	2020 (2)	RF	Standard SU

392 Note: LRA is the abbreviation of linear regression analysis.

393



394

395

396

Figure 8. Comparisons of different grazing datasets for the years 2001 and 2015: (a) spatial patterns; (b) predicted livestock number and census data at county scale; (c) accuracy evaluation between predicted livestock number and statistic data.

## 397 4.2 Spatial heterogeneity of grazing intensities

398 In general, the multiyear average grazing intensity on the QTP increased from west to east during  
399 1990 to 2020, with broad spatial heterogeneity (Figure 7). Highest grazing intensity was found mainly  
400 in the northeastern and south-central regions of the Plateau (mostly higher than 5.0 SU/hm<sup>2</sup>), while  
401 they were lowest in the northwest (mostly less than 1.0 SU/hm<sup>2</sup>). Over the past 31 years, the average  
402 grazing intensity decreased across most of the Plateau, but 36.05% of the entire QTP grassland still  
403 encountered continuous grazing intensity increase, especially in the northeastern regions (Figure 7).

404 The spatial heterogeneity of grazing intensities on the QTP may be attributed to the following  
405 reasons. First, complex geographic and climatic conditions on the QTP determine the heterogeneity of  
406 grassland, which in turn affects livestock distribution (Wang et al., 2018; Wei et al., 2022). In general,  
407 the grazing intensity patterns shown in the GDGI maps are basically consistent with the stocking rate  
408 threshold patterns in the QTP grasslands, both decreased from east to west (Zhu et al., 2023b). This  
409 phenomenon partially reflects the heterogeneity of the grasslands, as the alpine meadows and the  
410 steppes mainly distributed in the east and the west, respectively. Second, the dynamics of  
411 socio-economic development are obviously another important factors determining grazing intensity. In  
412 areas falling behind in terms of the socio-economic indicators, herders prefer to increase livestock in  
413 efforts to improve household incomes, leading to greater pressure on grasslands in these regions (Fang  
414 and Wu, 2022). In addition, the perceived increases in human population also resulted in the  
415 considerably increased need to more livestock (Wei et al., 2022). Third, the grazing intensity patterns  
416 across the QTP partially reflected the effects of management policies launched in different periods. For  
417 example, the grazing intensity on the QTP grassland increased substantially in the early 1990s, likely  
418 due to the launch of the household contract responsibility system. Moreover, the grazing intensity  
419 decreased in the late 1990s and early 2000s (Figure 7d), reflecting the implement of several strict  
420 ecological conservation programs, such as the grazing withdrawal program, conversion of cropland to  
421 grassland and ecological subsidy and award system. Finally, natural disasters have also been an  
422 important cause of the drastic reduction in livestock numbers. For example, the snow disasters that  
423 occurred in Naqu in 1997-1998, central Tibetan Plateau, resulted in the loss of 820,000 livestock (Ye et  
424 al., 2020).

## 425 4.3 Implications for grazing management

426 Nearly half of the grasslands on the QTP have been reported to be degraded over the past four  
427 decades (Wang et al., 2018; Dong et al., 2020), with some reports even indicating that the degraded  
428 grassland has reached 90% (Wang et al., 2021). It is widely recognized that overgrazing is the  
429 predominant and most pervasive unsustainable human activity continuing to drive grassland  
430 degradation on the QTP (Wang et al., 2018; Chen et al., 2019). Generally, these degraded grassland on  
431 the QTP can be effectively restored by adaptive management (Wang et al., 2022). However, better  
432 management of grasslands requires a deeper understanding of the anthropogenic activities, which still  
433 remain an important challenge and can be effectively addressed by the GDGI dataset.

434 According to the GDGI maps generated in this study, high-intensity grazing activities are mainly  
435 concentrated in the northeastern as well as the south-central part of the QTP, with the grazing intensity  
436 in some areas even nearly more than ten times than the average value of the entire plateau (Figure 5b),  
437 and have exceeded the stocking rate threshold of these grasslands (Zhu et al., 2023b). Population



438 growth and the related increasing livelihood demands is one of the main reasons for this increase. To  
439 meet daily needs and enhance household income, the herders have endeavored to increase livestock,  
440 thereby intensifying grazing pressures on the grasslands over the QTP (Abu Hammad and Tumeizi,  
441 2012; Fang and Wu, 2022). Although the current average grazing intensity in the northwest QTP  
442 (around 1.0 SU/hm<sup>2</sup>) is below their average stocking rate threshold (around 1.5 SU/hm<sup>2</sup>) (Zhu et al.,  
443 2023b), the grassland management should still be given adequate attention. Because as the most arid  
444 areas with low stocking rate threshold on the QTP, the grazing intensity in this region has been  
445 increasing in recent years. Nevertheless, it must be noted that the stocking rate threshold may exceed  
446 the carrying capacity, because it is predicted to lead to an extreme grassland degradation (Zhu et al.,  
447 2023b). The GDGI dataset also showed a similar pattern between the grazing intensity data and the  
448 WorldPop data near the built-up areas, indicating higher grazing intensity around settlements than other  
449 regions on the QTP. In addition, the GDGI dataset also indicate that from 1990 to 2020, although the  
450 grazing intensity of the Plateau has generally decreased, the hotspot areas for grazing activities have  
451 remained almost unchanged. This implies that these regions should be the focus of adaptive grassland  
452 management to effectively prevent grassland degradation, mainly based on the grass–livestock balance  
453 which varies by time and space.

454 Encouragingly, the GDGI dataset show that the grazing intensity for two-thirds of the entire QTP  
455 grassland decreased over the past 31 years, which is also consistent with other studies (Li et al., 2021;  
456 Sun et al., 2021). Recent decades of biodiversity protection, active restoration projects as well as  
457 management measures, such as nature reserves, grazing exclusion, part grazing ban combined with  
458 fencing enclosure, are believed to have driven these decrease (Deng et al., 2017; Li and Bennett, 2019).  
459 In addition, most grassland in the eastern Sanjiangyuan, the mid-eastern Changtang, and the northern  
460 foothills of the Himalayas, showed a significant decrease with grazing intensity (Figure 5e), indicating  
461 the importance of protected areas on preventing overstock and grassland degradation. Meanwhile, the  
462 GDGI maps also show that the grazing density varies greatly among protected areas, possibly owing to  
463 the difference in policy implementation. For instance, it can be seen from the GDGI maps that grazing  
464 intensity are increasing in some protected areas, especially several wetland nature reserves on the Zoige  
465 plateau (Figure 5e). Moreover, the average grazing intensity in all nature reserves on the QTP has  
466 overall increased from 1990 to 2020, although their increase rate is much lower than the non-protected  
467 areas (0.0125 SU/hm<sup>2</sup>·10a vs 0.0304 SU/hm<sup>2</sup>·10a), which implies that grassland management in  
468 protected areas still needs to be strengthened on the QTP.

469 The grazing initiatives in alignment with the Sustainable Development Goals (SDGs) on the QTP  
470 can benefit from the GDGI dataset. Firstly, determination a reasonable stocking rate is vital to prevent  
471 overstocking of the pastures, which will possibly induce extreme grassland degradation (Zhu et al.,  
472 2023b). Stocking rate determination can be optimized by using our grazing intensity maps and the  
473 stocking rate threshold maps of the QTP. Secondly, the GDGI maps can contribute to strategic  
474 placement of fence, which is a common practice adopted to prevent grassland degradation on the QTP.  
475 Building fences in areas with high grazing intensity and exceeding the carrying capacity can improve  
476 the effectiveness of fence construction (Zhang et al., 2023; Zhou et al., 2023). Thirdly, the GDGI  
477 dataset can provide a solid support for promoting effective nature reserve management, which in total  
478 covering nearly one third of the entire QTP. For example, the GDGI maps showed that grazing  
479 activities still exist in most nature reserves on the Plateau, although most of them have significantly  
480 lower grazing intensities compared with their adjacent non-protected areas. By using the GDGI maps,

481 the conflict between ecological protection and grazing activities in nature reserves can be alleviated.  
482 Finally, our grazing intensity maps can act as a basic dataset to support other grassland-related policies.  
483 Currently, these policies on the QTP often adopt a one-size-fits-all approach to determine the carrying  
484 capacity and carry out ecological compensation, which may lead to overstock or unfair financial  
485 distribution (Wang et al., 2022). The grassland management strategies balancing carrying capacity and  
486 stocking rates are more likely to result in optimal management choices for policymakers and  
487 stakeholders, and our GDGI maps can contribute to this decision-making processes.

#### 488 **4.4 Uncertainties and limitations**

489 Although this study has collected as reliable datasets as possible, users of the GDGI products  
490 should be cognizant of inherent uncertainties and limitations within these datasets. Notably, the mean  
491 relative error of the GDGI dataset spanning 1990 to 2020 was recorded at 4.2% (Figure 4a), calculated  
492 from the average errors across 182 counties within the QTP that had accessible livestock census data.  
493 Furthermore, approximately 8.26% of grassland areas exhibited a relative error exceeding 1.0 SU/hm<sup>2</sup>  
494 (Figure 4b). Such discrepancies arise from several limitations that were subsequently propagated to the  
495 final grazing intensity maps, thereby contributing to the dataset's overall uncertainties.

496 Firstly, the estimations of grazing intensities were fundamentally conservative, primarily due to the  
497 lack of comprehensive input data. Livestock numbers, derived from year-end data at the county level,  
498 inadvertently led to underestimations of grazing intensity by not accounting for livestock off-take rates.  
499 Likewise, the evaluation focused solely on livestock grazing intensity, excluding wild herbivores and  
500 forage-dependent livestock, which potentially underestimate actual grazing pressures on the QTP.  
501 Additionally, despite identifying seven main factors influencing livestock distribution, the study did not  
502 encompass all potential factors, such as fencing, forage availability, road proximity, and season  
503 transformation in grazing practices. Moreover, to align with county-scale livestock census data, we  
504 averaged the environmental factors at the county-scale. Although this approach have been widely used  
505 on the hypothesis that a consistent causal relationship between livestock intensity and environmental  
506 factors persists across various scales (Robinson et al., 2014; Nicolas et al., 2016; Li et al., 2021; Meng  
507 et al., 2023), it might oversimplify the intricate dynamics between grazing intensity and lead to a  
508 certain degree of estimation inaccuracies. In addition, the reliance on linear extrapolation to  
509 Supplementary missing gridded 100-m population density data from 1990-1999 introduced further  
510 uncertainties due to the limited resolution (1-km) and interval (5-year) of the ChinaPop dataset.

511 Secondly, the modeling process for mapping grazing intensity also suffered from several challenges.  
512 For instance, the ET model was trained with a limited sample size of 4,998 and applied to a vast area  
513 consisting of 150 million pixels, which could compromise the model's accuracy. In addition, despite the  
514 ET model's design to reduce overfitting risks by using randomly selected features and partition decision,  
515 the potential for overfit effects still remained, particularly when faced with a high number of output  
516 classes or insufficient sample sizes (Geurts et al., 2006; Galelli and Castelletti, 2013). In fact, this  
517 limitation was evident in this study, as the generalization capability of the ET model was restricted by  
518 the disparity between the number of training samples and the total number of pixels, leading to  
519 predictions that often exceeded actual livestock census (Figure 4a).

520 Thirdly, our methodological framework for high-resolution gridded grazing dataset mapping was  
521 developed based on the assumption that all grassland were accessible to livestock. However, in reality,  
522 the amount of available grassland was less due to fencing and grazing bans on the QTP (Zhan et al.,  
523 2023). Moreover, transhumant herders generally follow a seasonal calendar for summer pastures and

524 winter pastures on the QTP. However, we did not consider this seasonal movements due to data  
525 limitations, which further restrict the analysis of seasonal livestock distribution patterns (Kolluru et al.,  
526 2023). Additionally, the model's reliance on human population as a proxy for livestock locations  
527 overlooked the possibility of high grazing intensity in areas with low human populations on the QTP,  
528 particularly in regions designated for summer pastures.

529 In summary, all these limitations associated with input data, the modeling process, and the  
530 methodological framework collectively contribute to the uncertainties and reduce accuracy of the  
531 GDGI maps. We henceforth recommend that future research should aim to incorporate more detailed  
532 data, consider additional influential factors, enhance key dataset's time-series consistency, and refine  
533 the methodological framework to improve the accuracy of grazing intensity mapping.

## 534 **5 Data availability**

535 The annual gridded grazing intensity maps of the QTP spanning from 1990 to 2020 are accessible  
536 at the following link: <https://doi.org/10.5281/zenodo.10851119> (Zhou et al., 2024). Each map is  
537 catalogued by year and recorded in GeoTIFF format, with values represented in SU/hm<sup>2</sup> per year.  
538 These datasets, with a spatial resolution of 100 m and annual temporal resolution, utilize the  
539 WGS-1984-Albers geographic coordinate system. To streamline data transfer and download processes,  
540 the comprehensive 31-year dataset has been compressed into a ZIP file, readily available for download  
541 and compatible with Geographic Information System (GIS) software for viewing.

## 542 **6 Conclusions**

543 In this study, we introduce a framework utilizing ET machine learning algorithms to achieve  
544 fine-scale livestock spatialization, subsequently generating the GDGI dataset across the QTP. The  
545 GDGI has a spatial resolution of 100 m and expands 31 years from 1990 to 2020. It is consistent with  
546 livestock census data of the QTP, and has a relatively higher precision than previous datasets with  
547 MAE of 0.006 SU/hm<sup>2</sup> based on 4,998 independent test samples. In addition, the accuracy evaluations  
548 at both pixel-level and township-level underscore the outstanding reliability and applicability of the  
549 GDGI dataset, which can successfully capture the spatial heterogeneity and variation in grazing  
550 intensities in greater details. Moreover, comparisons between the GDGI dataset and other existing  
551 grazing map products further proved the robust and efficient of our dataset, and demonstrate the  
552 validity of the proposed framework in the research of livestock spatialization. The GDGI dataset  
553 presented in this study can address existing limitations and enhance the understanding of grazing  
554 activities on the QTP. This, in turn, can aid in the rational utilization of grasslands and facilitate the  
555 implementation of informed and sustainable management practices.

## 556 **Supplementary.**

557 For gridded datasets influencing grazing that are not directly available, or that do not meet  
558 spatio-temporal resolution requirements—such as those pertaining to population density, temperature,  
559 precipitation, and HNPP—we have delineated the processing or creation procedures in the  
560 Supplementary file.

561 **Author contributions.**

562 T.L. conceived the research; J.Z. and J.N. performed the analyses and wrote the first draft of the  
563 paper; N.W. and T.L. reviewed and edited the paper before submission. All authors made substantial  
564 contributions to the discussion of content.

565 **Competing interests.**

566 The authors declare that they have no conflict of interest.

567 **Acknowledgements.**

568 We would like to thank the Bureau of Statistics of each county over the QTP for providing the  
569 census livestock data.

570 **Financial support.**

571 This research was supported by the Second Tibetan Plateau Scientific Expedition and Research  
572 Program (STEP), Ministry of Science and Technology of the People's Republic of China (grant no.  
573 2019QZKK0402) and the National Natural Science Foundation of China (grant no. 42071238).  
574

575 **References**

- 576 Abu Hammad, A. and Tumeizi, A.: Land degradation: socioeconomic and environmental causes and  
577 consequences in the eastern Mediterranean, *Land. Degrad. Dev.*, 23, 216-226,  
578 <https://doi.org/10.1002/ldr.1069>, 2012.
- 579 Ahmad, M. W., Reynolds, J., and Rezgoui, Y.: Predictive modelling for solar thermal energy systems: A  
580 comparison of support vector regression, random forest, extra trees and regression trees, *J. Clean.*  
581 *Prod.*, 203, 810-821, <https://doi.org/10.1016/j.jclepro.2018.08.207>, 2018.
- 582 Allred, B. W., Fuhlendorf, S. D., Hovick, T. J., Dwayne Elmore, R., Engle, D. M., and Joern, A.:  
583 Conservation implications of native and introduced ungulates in a changing climate, *Glob. Chang.*  
584 *Biol.*, 19, 1875-1883, <https://doi.org/10.1111/gcb.12183>, 2013.
- 585 Breiman, L.: Random Forests, *Mach. Learn.*, 45, 5-32, <https://doi.org/10.1023/A:1010933404324>,  
586 2001.
- 587 Cai, Y., Wang, X., Tian, L., Zhao, H., Lu, X., and Yan, Y.: The impact of excretal returns from yak and  
588 Tibetan sheep dung on nitrous oxide emissions in an alpine steppe on the Qinghai-Tibetan Plateau,  
589 *Soil. Biol. Biochem.*, 76, 90-99, <https://doi.org/10.1016/j.soilbio.2014.05.008>, 2014.
- 590 Chang, J., Ciais, P., Gasser, T., Smith, P., Herrero, M., Havlík, P., Obersteiner, M., Guenet, B., Goll, D.  
591 S., Li, W., Naipal, V., Peng, S., Qiu, C., Tian, H., Viovy, N., Yue, C., and Zhu, D.: Climate warming  
592 from managed grasslands cancels the cooling effect of carbon sinks in sparsely grazed and natural  
593 grasslands, *Nat. Commun.*, 12, 118, <https://doi.org/10.1038/s41467-020-20406-7>, 2021.
- 594 Chen, Y., Ju, W., Mu, S., Fei, X., Cheng, Y., Propastin, P., Zhou, W., Liao, C., Chen, L., Tang, R., Qi, J.,  
595 Li, J., and Ruan, H.: Explicit Representation of Grazing Activity in a Diagnostic Terrestrial Model: A  
596 Data - Process Combined Scheme, *J. Adv. Model. Earth. Sy.*, 11, 957-978,  
597 <https://doi.org/10.1029/2018ms001352>, 2019.

598 Cortes, C. and Vapnik, V.: Support-vector networks, *Mach. Learn.*, 20, 273-297,  
599 <https://doi.org/10.1007/BF00994018>, 1995.

600 Cover, T. and Hart, P.: Nearest neighbor pattern classification, *Ieee. T. Inform. Theory.*, 13, 21-27,  
601 <https://doi.org/10.1109/TIT.1967.1053964>, 1967.

602 Dara, A., Baumann, M., Freitag, M., Hölzel, N., Hostert, P., Kamp, J., Müller, D., Prishchepov, A. V.,  
603 and Kuemmerle, T.: Annual Landsat time series reveal post-Soviet changes in grazing pressure,  
604 *Remote. Sens. Environ.*, 239, 111667, <https://doi.org/10.1016/j.rse.2020.111667>, 2020.

605 Deng, L., Shanguan, Z.-P., Wu, G.-L., and Chang, X.-F.: Effects of grazing exclusion on carbon  
606 sequestration in China's grassland, *Earth-Sci. Rev.*, 173, 84-95,  
607 <https://doi.org/10.1016/j.earscirev.2017.08.008>, 2017.

608 Dong, S., Shang, Z., Gao, J., and Boone, R. B.: Enhancing sustainability of grassland ecosystems  
609 through ecological restoration and grazing management in an era of climate change on  
610 Qinghai-Tibetan Plateau, *Agr. Ecosyst. Environ.*, 287, 106684,  
611 <https://doi.org/10.1016/j.agee.2019.106684>, 2020.

612 Fang, X. and Wu, J.: Causes of overgrazing in Inner Mongolian grasslands: Searching for deep  
613 leverage points of intervention, *Ecol. Soc.*, 27, <https://doi.org/10.5751/es-12878-270108>, 2022.

614 Feng, R., Long, R., Shang, Z., Ma, Y., Dong, S., and Wang, Y.: Establishment of *Elymus natans*  
615 improves soil quality of a heavily degraded alpine meadow in Qinghai-Tibetan Plateau, China, *Plant.*  
616 *Soil.*, 327, 403-411, <https://doi.org/10.1007/s11104-009-0065-3>, 2009.

617 Fetzl, T., Havlik, P., Herrero, M., Kaplan, J. O., Kastner, T., Kroisleitner, C., Rolinski, S., Searchinger,  
618 T., Van Bodegom, P. M., Wirsenius, S., and Erb, K. H.: Quantification of uncertainties in global  
619 grazing systems assessment, *Global. Biogeochem. Cy.*, 31, 1089-1102,  
620 <https://doi.org/10.1002/2016gb005601>, 2017.

621 Friedman, J. H.: Greedy function approximation: a gradient boosting machine, *Ann. Stat.*, 29,  
622 1189-1232, <https://doi.org/10.1214/aos/1013203451>, 2001.

623 Galelli, S. and Castelletti, A.: Assessing the predictive capability of randomized tree-based ensembles  
624 in streamflow modelling, *Hydrol. Earth. Syst. Sc.*, 17, 2669-2684,  
625 <https://10.5194/hess-17-2669-2013>, 2013.

626 García-Ruiz, J. M., Tomás-Faci, G., Diarte-Blasco, P., Montes, L., Domingo, R., Sebastián, M., Lasanta,  
627 T., González-Sampériz, P., López-Moreno, J. I., Arnáez, J., and Beguería, S.: Transhumance and  
628 long-term deforestation in the subalpine belt of the central Spanish Pyrenees: An interdisciplinary  
629 approach, *Catena.*, 195, 104744, <https://doi.org/10.1016/j.catena.2020.104744>, 2020.

630 García, R., Aguilar, J., Toro, M., Pinto, A., and Rodríguez, P.: A systematic literature review on the use  
631 of machine learning in precision livestock farming, *Comput. Electron. Agr.*, 179, 105826,  
632 <https://doi.org/10.1016/j.compag.2020.105826>, 2020.

633 Garrett, R. D., Koh, I., Lambin, E. F., le Polain de Waroux, Y., Kastens, J. H., and Brown, J. C.:  
634 Intensification in agriculture-forest frontiers: Land use responses to development and conservation  
635 policies in Brazil, *Global. Environ. Chang.*, 53, 233-243,  
636 <https://doi.org/10.1016/j.gloenvcha.2018.09.011>, 2018.

637 Geurts, P., Ernst, D., and Wehenkel, L.: Extremely randomized trees, *Mach. Learn.*, 63, 3-42,  
638 <https://doi.org/10.1007/s10994-006-6226-1>, 2006.

639 Gilbert, M., Nicolas, G., Cinardi, G., Van Boeckel, T. P., Vanwambeke, S. O., Wint, G. R. W., and  
640 Robinson, T. P.: Global distribution data for cattle, buffaloes, horses, sheep, goats, pigs, chickens and  
641 ducks in 2010, *Sci. Data.*, 5, 180227, <https://doi.org/10.1038/sdata.2018.227>, 2018.

642 Godfray, H. C. J., Aveyard, P., Garnett, T., Hall, J. W., Key, T. J., Lorimer, J., Pierrehumbert, R. T.,  
643 Scarborough, P., Springmann, M., and Jebb, S. A.: Meat consumption, health, and the environment,  
644 *Science.*, 361, 243, <https://doi.org/10.1126/science.aam5324>, 2018.

645 Guo, Z., Li, Z., and Cui, G.: Effectiveness of national nature reserve network in representing natural  
646 vegetation in mainland China, *Biodivers. Conserv.*, 24, 2735-2750,  
647 <https://doi.org/10.1007/s10531-015-0959-8>, 2015.

648 Han, Y., Dong, S., Zhao, Z., Sha, W., Li, S., Shen, H., Xiao, J., Zhang, J., Wu, X., Jiang, X., Zhao, J.,  
649 Liu, S., Dong, Q., Zhou, H., and Yeomans, J. C.: Response of soil nutrients and stoichiometry to  
650 elevated nitrogen deposition in alpine grassland on the Qinghai-Tibetan Plateau, *Geoderma.*, 343,  
651 263-268, <https://doi.org/10.1016/j.geoderma.2018.12.050>, 2019.

652 He, M., Pan, Y., Zhou, G., Barry, K. E., Fu, Y., and Zhou, X.: Grazing and global change factors  
653 differentially affect biodiversity - ecosystem functioning relationships in grassland ecosystems, *Glob.*  
654 *Chang. Biol.*, 28, 5492-5504, <https://doi.org/10.1111/gcb.16305>, 2022.

655 Heddam, S., Ptak, M., and Zhu, S.: Modelling of daily lake surface water temperature from air  
656 temperature: Extremely randomized trees (ERT) versus Air2Water, MARS, M5Tree, RF and  
657 MLPNN, *J. Hydrol.*, 588, 125130, <https://doi.org/10.1016/j.jhydrol.2020.125130>, 2020.

658 Hu, Y., Cheng, H., and Tao, S.: Environmental and human health challenges of industrial livestock and  
659 poultry farming in China and their mitigation, *Environ. Int.*, 107, 111-130,  
660 <https://doi.org/10.1016/j.envint.2017.07.003>, 2017.

661 Huang, X., Yang, Y., Chen, C., Zhao, H., Yao, B., Ma, Z., Ma, L., and Zhou, H.: Quantifying and  
662 Mapping Human Appropriation of Net Primary Productivity in Qinghai Grasslands in China,  
663 *Agriculture.*, 12, 483, <https://doi.org/10.3390/agriculture12040483>, 2022.

664 Humpenöder, F., Bodirsky, B. L., Weindl, I., Lotze-Campen, H., Linder, T., and Popp, A.: Projected  
665 environmental benefits of replacing beef with microbial protein, *Nature.*, 605, 90-96,  
666 <https://doi.org/10.1038/s41586-022-04629-w>, 2022.

667 Jiang, M., Zhao, X., Wang, R., Yin, L., and Zhang, B.: Assessment of Conservation Effectiveness of the  
668 Qinghai-Tibet Plateau Nature Reserves from a Human Footprint Perspective with Global Lessons,  
669 *Land.*, 12, 869, <https://doi.org/10.3390/land12040869>, 2023.

670 Kolluru, V., John, R., Saraf, S., Chen, J., Hankerson, B., Robinson, S., Kussainova, M., Jain, K.:  
671 Gridded livestock density database and spatial trends for Kazakhstan, *Sci Data.*, 10(1), 839,  
672 10.1038/s41597-023-02736-5, 2023.

673 Kumar, P., Abubakar, A. A., Verma, A. K., Umaraw, P., Adewale Ahmed, M., Mehta, N., Nizam Hayat,  
674 M., Kaka, U., and Sazili, A. Q.: New insights in improving sustainability in meat production:  
675 opportunities and challenges, *Crit .Rev. Food. Sci.*, 1-29,  
676 <https://doi.org/10.1080/10408398.2022.2096562>, 2022.

677 Li, M., Liu, S., Wang, F., Liu, H., Liu, Y., and Wang, Q.: Cost-benefit analysis of ecological restoration  
678 based on land use scenario simulation and ecosystem service on the Qinghai-Tibet Plateau, *Glob.*  
679 *Ecol. Conserv.*, 34, e02006, <https://doi.org/10.1016/j.gecco.2022.e02006>, 2022a.

680 Li, P. and Bennett, J.: Understanding herders' stocking rate decisions in response to policy initiatives,  
681 *Sci. Total. Environ.*, 672, 141-149, <https://doi.org/10.1016/j.scitotenv.2019.03.407>, 2019.

682 Li, Q., Zhang, C., Shen, Y., Jia, W., and Li, J.: Quantitative assessment of the relative roles of climate  
683 change and human activities in desertification processes on the Qinghai-Tibet Plateau based on net  
684 primary productivity, *Catena.*, 147, 789-796, <https://doi.org/10.1016/j.catena.2016.09.005>, 2016.

685 Li, T., Cai, S., Singh, R. K., Cui, L., Fava, F., Tang, L., Xu, Z., Li, C., Cui, X., Du, J., Hao, Y., Liu, Y.,

686 and Wang, Y.: Livelihood resilience in pastoral communities: Methodological and field insights from  
687 Qinghai-Tibetan Plateau, *Sci. Total. Environ.*, 838, 155960,  
688 <https://doi.org/10.1016/j.scitotenv.2022.155960>, 2022b.

689 Li, X., Hou, J., and Huang, C.: High-Resolution Gridded Livestock Projection for Western China Based  
690 on Machine Learning, *Remote. Sens.*, 13, 5038, <https://doi.org/10.3390/rs13245038>, 2021.

691 Lin, G., Lin, A., and Gu, D.: Using support vector regression and K-nearest neighbors for short-term  
692 traffic flow prediction based on maximal information coefficient, *Inform. Sciences.*, 608, 517-531,  
693 <https://doi.org/10.1016/j.ins.2022.06.090>, 2022.

694 Liu, B. T.: Actual livestock carrying capacity estimation product in Qinghai-Tibet Plateau (2000-2019),  
695 National Tibetan Plateau Data Center. [Dataset], <https://doi.org/10.11888/Ecolo.tpdc.271513>, 2021.

696 Long, S., Wei, X., Zhang, F., Zhang, R., Xu, J., Wu, K., Li, Q., and Li, W.: Estimating daily  
697 ground-level NO<sub>2</sub> concentrations over China based on TROPOMI observations and machine  
698 learning approach, *Atmos. Environ.*, 289, 119310, <https://doi.org/10.1016/j.atmosenv.2022.119310>,  
699 2022.

700 Luo, J., Hoogendoorn, C., van der Weerden, T., Saggart, S., de Klein, C., Giltrap, D., Rollo, M., and Rys,  
701 G.: Nitrous oxide emissions from grazed hill land in New Zealand, *Agr. Ecosyst. Environ.*, 181,  
702 58-68, <https://doi.org/10.1016/j.agee.2013.09.020>, 2013.

703 Ma, C., Xie, Y., Duan, H., Wang, X., Bie, Q., Guo, Z., He, L., and Qin, W.: Spatial quantification  
704 method of grassland utilization intensity on the Qinghai-Tibetan Plateau: A case study on the Selinco  
705 basin, *J. Environ. Manage.*, 302, 114073, <https://doi.org/10.1016/j.jenvman.2021.114073>, 2022.

706 Mack, G., Walter, T., and Flury, C.: Seasonal alpine grazing trends in Switzerland: Economic  
707 importance and impact on biotic communities, *Environ. Sci. Policy.*, 32, 48-57,  
708 <https://doi.org/10.1016/j.envsci.2013.01.019>, 2013.

709 Martinuzzi, S., Radeloff, V. C., Pastur, G. M., Rosas, Y. M., Lizarraga, L., Politi, N., Rivera, L., Herrera,  
710 A. H., Silveira, E. M. O., Olah, A., and Pidgeon, A. M.: Informing forest conservation planning with  
711 detailed human footprint data for Argentina, *Glob. Ecol. Conserv.*, 31, e01787,  
712 <https://doi.org/10.1016/j.gecco.2021.e01787>, 2021.

713 McSherry, M. E. and Ritchie, M. E.: Effects of grazing on grassland soil carbon: a global review, *Glob.*  
714 *Chang. Biol.*, 19, 1347-1357, <https://doi.org/10.1111/gcb.12144>, 2013.

715 Meng, N., Wang, L., Qi, W., Dai, X., Li, Z., Yang, Y., Li, R., Ma, J., and Zheng, H.: A high-resolution  
716 gridded grazing dataset of grassland ecosystem on the Qinghai-Tibet Plateau in 1982-2015, *Sci.*  
717 *Data.*, 10, 68, <https://doi.org/10.1038/s41597-023-01970-1>, 2023.

718 Miao, L., Sun, Z., Ren, Y., Schierhorn, F., and Müller, D.: Grassland greening on the Mongolian  
719 Plateau despite higher grazing intensity, *Land. Degrad. Dev.*, 32, 792-802,  
720 <https://doi.org/10.1002/ldr.3767>, 2020.

721 Minoofar, A., Gholami, A., Eslami, S., Hajizadeh, A., Gholami, A., Zandi, M., Ameri, M., and Kazem,  
722 H. A.: Renewable energy system opportunities: A sustainable solution toward cleaner production and  
723 reducing carbon footprint of large-scale dairy farms, *Energ. Convers. Manage.*, 293, 117554,  
724 <https://doi.org/10.1016/j.enconman.2023.117554>, 2023.

725 Mulligan, M., van Soesbergen, A., Hole, D. G., Brooks, T. M., Burke, S., and Hutton, J.: Mapping  
726 nature's contribution to SDG 6 and implications for other SDGs at policy relevant scales, *Remote.*  
727 *Sens. Environ.*, 239, 111671, <https://doi.org/10.1016/j.rse.2020.111671>, 2020.

728 Muloi, D. M., Wee, B. A., McClean, D. M. H., Ward, M. J., Pankhurst, L., Phan, H., Ivens, A. C.,  
729 Kivali, V., Kiyong'a, A., Ndinda, C., Gitahi, N., Ouko, T., Hassell, J. M., Imboma, T., Akoko, J.,

730 Murungi, M. K., Njoroge, S. M., Muinde, P., Nakamura, Y., Alumasa, L., Furmaga, E., Kaitho, T.,  
731 Öhgren, E. M., Amana, F., Ogendo, A., Wilson, D. J., Bettridge, J. M., Kiiru, J., Kyobutungi, C.,  
732 Tacoli, C., Kang'ethe, E. K., Davila, J. D., Kariuki, S., Robinson, T. P., Rushton, J., Woolhouse, M. E.  
733 J., and Fèvre, E. M.: Population genomics of *Escherichia coli* in livestock-keeping households across  
734 a rapidly developing urban landscape, *Nat. Microbiol.*, 7, 581-589,  
735 <https://doi.org/10.1038/s41564-022-01079-y>, 2022.

736 Neumann, K., Elbersen, B. S., Verburg, P. H., Staritsky, I., Pérez-Soba, M., de Vries, W., and Rienks, W.  
737 A.: Modelling the spatial distribution of livestock in Europe, *Landscape. Ecol.*, 24, 1207-1222,  
738 <https://doi.org/10.1007/s10980-009-9357-5>, 2009.

739 Nicolas, G., Robinson, T. P., Wint, G. R., Conchedda, G., Cinardi, G., and Gilbert, M.: Using Random  
740 Forest to Improve the Downscaling of Global Livestock Census Data, *Plos. One.*, 11, e0150424,  
741 <https://doi.org/10.1371/journal.pone.0150424>, 2016.

742 O'Neill, D. W. and Abson, D. J.: To settle or protect? A global analysis of net primary production in  
743 parks and urban areas, *Ecol. Econ.*, 69, 319-327, <https://doi.org/10.1016/j.ecolecon.2009.08.028>,  
744 2009.

745 Pan, Y., Chen, S., Qiao, F., Ukkusuri, S. V., and Tang, K.: Estimation of real-driving emissions for  
746 buses fueled with liquefied natural gas based on gradient boosted regression trees, *Sci. Total.*  
747 *Environ.*, 660, 741-750, <https://doi.org/10.1016/j.scitotenv.2019.01.054>, 2019.

748 Petz, K., Alkemade, R., Bakkenes, M., Schulp, C. J. E., van der Velde, M., and Leemans, R.: Mapping  
749 and modelling trade-offs and synergies between grazing intensity and ecosystem services in  
750 rangelands using global-scale datasets and models, *Global. Environ. Chang.*, 29, 223-234,  
751 <https://doi.org/10.1016/j.gloenvcha.2014.08.007>, 2014.

752 Pozo, R. A., Cusack, J. J., Acebes, P., Malo, J. E., Traba, J., Iranzo, E. C., Morris-Trainor, Z.,  
753 Minderman, J., Bunnefeld, N., Radic-Schilling, S., Moraga, C. A., Arriagada, R., and Corti, P.:  
754 Reconciling livestock production and wild herbivore conservation: challenges and opportunities,  
755 *Trends. Ecol. Evol.*, 36, 750-761, <https://doi.org/10.1016/j.tree.2021.05.002>, 2021.

756 Prosser, D. J., Wu, J., Ellis, E. C., Gale, F., Van Boeckel, T. P., Wint, W., Robinson, T., Xiao, X., and  
757 Gilbert, M.: Modelling the distribution of chickens, ducks, and geese in China, *Agric Ecosyst*  
758 *Environ.*, 141, 381-389, <https://doi.org/10.1016/j.agee.2011.04.002>, 2011.

759 Robinson, T. P., Wint, G. R., Conchedda, G., Van Boeckel, T. P., Ercoli, V., Palamara, E., Cinardi, G.,  
760 D'Aiatti, L., Hay, S. I., and Gilbert, M.: Mapping the global distribution of livestock, *Plos. One.*, 9,  
761 e96084, <https://doi.org/10.1371/journal.pone.0096084>, 2014.

762 Rokach, L.: Decision forest: Twenty years of research, *Inform. Fusion.*, 27, 111-125,  
763 <https://doi.org/10.1016/j.inffus.2015.06.005>, 2016.

764 Shakoob, A., Shakoob, S., Rehman, A., Ashraf, F., Abdullah, M., Shahzad, S. M., Farooq, T. H., Ashraf,  
765 M., Manzoor, M. A., Altaf, M. M., and Altaf, M. A.: Effect of animal manure, crop type, climate  
766 zone, and soil attributes on greenhouse gas emissions from agricultural soils-A global meta-analysis,  
767 *J. Clean. Prod.*, 278, 124019, <https://doi.org/10.1016/j.jclepro.2020.124019>, 2021.

768 Sun, J., Liu, M., Fu, B., Kemp, D., Zhao, W., Liu, G., Han, G., Wilkes, A., Lu, X., Chen, Y., Cheng, G.,  
769 Zhou, T., Hou, G., Zhan, T., Peng, F., Shang, H., Xu, M., Shi, P., He, Y., Li, M., Wang, J., Tsunekawa,  
770 A., Zhou, H., Liu, Y., Li, Y., and Liu, S.: Reconsidering the efficiency of grazing exclusion using  
771 fences on the Tibetan Plateau, *Sci. Bull.*, 65, 1405-1414, <https://doi.org/10.1016/j.scib.2020.04.035>,  
772 2020.

773 Sun, Y., Liu, S., Liu, Y., Dong, Y., Li, M., An, Y., and Shi, F.: Grazing intensity and human activity



774 intensity data sets on the Qinghai - Tibetan Plateau during 1990 - 2015, *Geoscience. Data. Journal*,  
775 9, 140-153, <https://doi.org/10.1002/gdj3.127>, 2021.

776 Tabassum, A., Abbasi, T., and Abbasi, S. A.: Reducing the global environmental impact of livestock  
777 production: the minilivestock option, *J. Clean. Prod.*, 112, 1754-1766,  
778 <https://doi.org/10.1016/j.jclepro.2015.02.094>, 2016.

779 Van Boeckel, T. P., Prosser, D., Franceschini, G., Biradar, C., Wint, W., Robinson, T., and Gilbert, M.:  
780 Modelling the distribution of domestic ducks in Monsoon Asia, *Agr. Ecosyst. Environ.*, 141, 373-380,  
781 <https://doi.org/10.1016/j.agee.2011.04.013>, 2011.

782 Veldhuis, M. P., Ritchie, M. E. O., Joseph O., Morrison, T. A., Beale, C. M., Estes, A. B., Mwakilema,  
783 W., Ojwang, G. O. P., Catherine L., Probert, J., Wargute, P. W., Hopcraft, J. G. C., and Olf, H.:  
784 Cross-boundary human impacts compromise the Serengeti-Mara ecosystem, *Science.*, 363,  
785 1424-1428, <https://doi.org/10.1126/science.aav0564>, 2019.

786 Venglovsky, J., Sasakova, N., and Placha, I.: Pathogens and antibiotic residues in animal manures and  
787 hygienic and ecological risks related to subsequent land application, *Bioresour. Technol.*, 100,  
788 5386-5391, <https://doi.org/10.1016/j.biortech.2009.03.068>, 2009.

789 Waha, K., van Wijk, M. T., Fritz, S., See, L., Thornton, P. K., Wichern, J., and Herrero, M.: Agricultural  
790 diversification as an important strategy for achieving food security in Africa, *Glob. Chang. Biol.*, 24,  
791 3390-3400, <https://doi.org/10.1111/gcb.14158>, 2018.

792 Wang, R., Feng, Q., Jin, Z., and Liang, T.: The Restoration Potential of the Grasslands on the Tibetan  
793 Plateau, *Remote. Sens.*, 14, 80, <https://doi.org/10.3390/rs14010080>, 2021.

794 Wang, Y., Sun, Y., Wang, Z., Chang, S., and Hou, F.: Grazing management options for restoration of  
795 alpine grasslands on the Qinghai - Tibet Plateau, *Ecosphere.*, 9, e02515,  
796 <https://doi.org/10.1002/ecs2.2515>, 2018.

797 Wang, Y., Lv, W., Xue, K., Wang, S., Zhang, L., Hu, R., Zeng, H., Xu, X., Li, Y., Jiang, L., Hao, Y., Du,  
798 J., Sun, J., Dorji, T., Piao, S., Wang, C., Luo, C., Zhang, Z., Chang, X., Zhang, M., Hu, Y., Wu, T.,  
799 Wang, J., Li, B., Liu, P., Zhou, Y., Wang, A., Dong, S., Zhang, X., Gao, Q., Zhou, H., Shen, M.,  
800 Wilkes, A., Mieke, G., Zhao, X., and Niu, H.: Grassland changes and adaptive management on the  
801 Qinghai-Tibetan Plateau, *Nat. Rev. Earth. Env.*, 3, 668-683,  
802 <https://doi.org/10.1038/s43017-022-00330-8>, 2022.

803 Wei, Y., Lu, H., Wang, J., Wang, X., and Sun, J.: Dual Influence of Climate Change and Anthropogenic  
804 Activities on the Spatiotemporal Vegetation Dynamics Over the Qinghai-Tibetan Plateau From 1981  
805 to 2015, *Earth's Future.*, 10, 1-23, <https://doi.org/10.1029/2021EF002566>, 2022.

806 Yang, J. and Huang, X.: The 30 m annual land cover dataset and its dynamics in China from 1990 to  
807 2019, *Earth. Syst. Sci. Data.*, 13, 3907-3925, <https://doi.org/10.5194/essd-13-3907-2021>, 2021.

808 Ye, T., Liu, W., Mu, Q., Zong, S., Li, Y. and Shi, P.: Quantifying livestock vulnerability to snow  
809 disasters in the Tibetan Plateau: Comparing different modeling techniques for prediction. *Int. J.*  
810 *Disaster Risk Reduct.*, 48, 101578, <https://doi.org/10.1016/j.ijdrr.2020.101578>, 2020.

811 Zhai, D., Gao, X., Li, B., Yuan, Y., Jiang, Y., Liu, Y., Li, Y., Li, R., Liu, W., and Xu, J.: Driving  
812 Climatic Factors at Critical Plant Developmental Stages for Qinghai-Tibet Plateau Alpine Grassland  
813 Productivity, *Remote. Sens.*, 14, 1564, <https://doi.org/10.3390/rs14071564>, 2022.

814 Zhan, N., Liu, W., Ye, T., Li, H., Chen, S., and Ma, H.: High-resolution livestock seasonal distribution  
815 data on the Qinghai-Tibet Plateau in 2020, *Sci. Data.*, 10, 142,  
816 <https://doi.org/10.1038/s41597-023-02050-0>, 2023.

817 Zhang, B., Zhang, Y., Wang, Z., Ding, M., Liu, L., Li, L., Li, S., Liu, Q., Paudel, B., and Zhang, H.:

818 Factors Driving Changes in Vegetation in Mt. Qomolangma (Everest): Implications for the  
819 Management of Protected Areas, *Remote. Sens.*, 13, 4725, <https://doi.org/10.3390/rs13224725>,  
820 2021a.

821 Zhang, R., Wang, Z., Han, G., Schellenberg, M. P., Wu, Q., and Gu, C.: Grazing induced changes in  
822 plant diversity is a critical factor controlling grassland productivity in the Desert Steppe, Northern  
823 China, *Agr. Ecosyst. Environ.*, 265, 73-83, <https://doi.org/10.1016/j.agee.2018.05.014>, 2018.

824 Zhang, W., Li, J., Struik, P. C., Jin, K., Ji, B., Jiang, S., Zhang, Y., Li, Y., Yang, X., and Wang, Z.:  
825 Recovery through proper grazing exclusion promotes the carbon cycle and increases carbon  
826 sequestration in semiarid steppe, *Sci. Total. Environ.*, 892, 164423,  
827 <https://doi.org/10.1016/j.scitotenv.2023.164423>, 2023.

828 Zhang, Y., Hu, Q., and Zou, F.: Spatio-Temporal Changes of Vegetation Net Primary Productivity and  
829 Its Driving Factors on the Qinghai-Tibetan Plateau from 2001 to 2017, *Remote. Sens.*, 13, 1566,  
830 <https://doi.org/10.3390/rs13081566>, 2021b.

831 Zhao, X., Xu, T., Ellis, J., He, F., Hu, L., and Li, Q.: Rewilding the wildlife in Sangjiangyuan National  
832 Park, Qinghai-Tibetan Plateau, *Ecosyst. Health. Sust.*, 6, 1776643,  
833 <https://doi.org/10.1080/20964129.2020.1776643>, 2020.

834 Zhou, J., Niu, J., Wu, N., and Lu, T.: Annual high-resolution grazing intensity maps on the  
835 Qinghai-Tibet Plateau from 1990 to 2020, Zenodo, <https://doi.org/10.5281/zenodo.10851119>, 2024.

836 Zhou, W., Li, C., Wang, S., Ren, Z., and Stringer, L. C.: Effects of grazing and enclosure management  
837 on soil physical and chemical properties vary with aridity in China's drylands, *Sci. Total. Environ.*,  
838 877, 162946, <https://doi.org/10.1016/j.scitotenv.2023.162946>, 2023.

839 Zhu, Y., Zhang, H., Ding, M., Li, L., and Zhang, Y.: The multiple perspective response of vegetation to  
840 drought on the Qinghai-Tibetan Plateau, *Remote. Sens.*, 15, 902, <https://doi.org/10.3390/rs15040902>,  
841 2023a.

842 Zhu, Q., Chen, H., Peng, C., Liu, J., Piao, S., He, J.-S., Wang, S., Zhao, X., Zhang, J., Fang, X., Jin, J.,  
843 Yang, Q.E., Ren, L., and Wang, Y.: An early warning signal for grassland degradation on the  
844 Qinghai-Tibetan Plateau, *Nat. Commun.*, 14, 6406, <https://doi.org/10.1038/s41467-023-42099-4>,  
845 2023b.